WOOD RESEARCH
64 (3): 2019
449-460

VARIATION IN THE CHARRING DEPTH OF WOOD STUDS INSIDE WOOD-FRAME WALLS WITH TIME IN A FIRE

Hung-Chi Su
Architecture and Building Research Institute, Ministry of the Interior
New Taipei City, Taiwan

Shu-Fen Tung, Chun-Ta Tzeng
National Cheng Kung University, Department of Architecture
Tainan City, Taiwan

Chi-Ming Lai
National Cheng Kung University, Department of Civil Engineering
Tainan City, Taiwan

(Received July 2018)

ABSTRACT

In this study, the variation in the charring depth of wood studs inside wood-frame walls (WFWs) in a fire was investigated. First, the time variation in the surface temperature of wood studs inside WFWs was determined based on ISO 834 fire-resistance tests, and the resulting heating conditions were used in subsequent heat exposure tests. Then, wood stud specimens of four different wood species (Chinese fir, Japanese cedar, Southern pine and spruce) were each subjected to a heat exposure test in an electric furnace. The results exhibited no significant correlation between the charring depth of the wood stud specimens and the preheating density. In addition, the test data validated that the equation proposed by Sugahara can be used for predicting the charring depth of wood studs inside WFWs in a fire.

KEYWORDS: Fire, char, wood-frame wall, stud, wood.

INTRODUCTION

Wood-frame walls (WFWs) commonly seen in practice, consist of wood studs, covering panels, insulation materials in joist and stud cavities, and fasteners. The constituent parts with standardized sizes and modules are fabricated in factories and assembled at construction sites to

save material, construction costs and promote construction quality. For WFWs, fire resistance is critical and important due to the reduction of the cross-sections of wood studs and the strength and stiffness of the heated zone when exposed to fire (Östman et al. 2017). To evaluate the fire resistance of WFWs, it is therefore necessary to predict the thermal degradation (charring) of wood studs.

Wood charring studies can be classified into several types based on the fire source (Babrauskas 2005): (1) those in which the specimen is heated with a heat flux generated at the specimen boundary using a cone calorimeter or other bench-scale tests, (2) those in which the specimen is heated in an ASTM E 119 or ISO 834 fire endurance test furnace using the provided time-temperature variation curve, and (3) those in which the charring of wood is observed in room (or multi-room) fire or a building fire.

Using cone calorimeter tests, Xu et al. (2015) examined the charring properties of five common timber species, three of which were softwood species (Douglas fir (*Pseudotsuga menziesii*), Scots pine (*Pinus sylvestris*) and Southern pine (genus *Pinus*)) and two of which were hardwood species (Shorea (a species of the genus Dipterocarpaceae) and merbau (*Intsia bijuga*)). It found that except for the merbau specimens, the equations recommended by the Eurocode 5, EC and the Australian Standard AS 1720.4 both underestimated the charring depth of the specimens.

Frangi et al. (2008) performed an extensive finite element-thermal analysis of timber beams initially protected by fire protection cladding based on the ISO 834 fire-resistance tests. They exposed these timber beams to a fire on three sides after the protection cladding fell off as a result of fire exposure (post-protection phase). Additionally, they proposed a charring model for timber frame floor assemblies with void cavities. Peng et al. (2010) reviewed fire-resistance tests of double shear timber connections. Their study subjects included wood-wood-wood connections with nails, bolts and dowels and wood-steel-wood connections with bolts and dowels. The results obtained from the ISO 834 fire-resistance tests were in good agreement with those obtained using the methodology recommended in the article. The measured upper gas layer temperatures closely reproduced the Eurocode 1 and ISO 834 time-temperature curves for compartment fires. Lineham et al. (2016) performed a series of fire tests on cross-laminated timber beams under sustained flexural loading using radiant heat generated from propane combustion as the fire source to provide constant heat flux conditions, which allowed for the continuous combustion of the specimens. They found that the discrepancies between predicted and observed responses in the tests described therein arose from incorrectly approximating the charring depth with heating.

Kolaitis et al. (2014) assessed the suitability of gypsum plasterboard and wood-based panels as fire protection cladding for light and massive timber elements using a compartment fire test.

Li et al. (2014) determined the origins of flashovers in large-scale compartments made of medium-density fiberboard based on the char pattern and depth and found that char layer and total thickness in the flame regions were deeper and thinner, respectively, than the rest of the compartment. Babrauskas (2005) analyzed the role of wood charring in fire investigations based on published test results and noted that for wood members without gaps or joints, the charring rates in a room fire were very close to those obtained from fire-resistance tests, but floors and other assemblies without solidly glued or laminated joints had relatively high charring rates. In addition, Babrauskas (2005) also comprehensively reviewed studies of wood charring. Jefimovas et al. (2017) proposed prediction equations for the local pyrolytic char duration and the local temperature of a standard fire based on electrical conductivity and electrical capacity measurements.

In this study, to determine the variation in the charring depth of wood studs in WFWs when exposed to a fire, wood stud specimens made of four wood species were each subjected to a heat exposure test under varying temperature conditions, which were set based on the ISO 834 Fire-resistance test results for WFWs.

MATERIAL AND METHODS

Determination of temperature boundary conditions for the principal test of wood stud specimens

Preliminary test specimens and heating conditions

In this study, the transient temperature distribution in wood studs in WFWs was determined by fire-resistance tests, which were used as the heating conditions for the subsequent principal test (Next section "The principal test"). During the fire-resistance tests, the heating conditions inside the furnace were set based on the heating curves specified in the ISO 834-1: 1999 Fire-resistance tests – Elements of building construction – Part 1: General requirements and the ISO 834-8: 2002 Fire-resistance tests – Elements of building construction – Part 8: Specific requirements for non-load bearing vertical separating elements. The specimens were heated for 60 min. Four full-scale WFW specimens of various sizes were prepared with two types of covering boards (gypsum and calcium silicate boards) and studs of two sizes (38 x 89 mm and 38 x 140 mm). Fig. 1 shows the specimens and the locations of thermocouples (marked ① and ②). Tab. 1 shows the structural details of the WFW specimens. Fig. 2 shows the ISO 834 furnace used in this study. The device is located in the Fire Experiment Center, Architecture & Building Research Institute, Ministry of Interior, on the Gueiren Campus of National Cheng Kung University, Taiwan.

Tab. 1: Details of the pretest specimens.

Specimen No.	A	B	C	D
Species of the stud	Spruce (SPF)	Spruce (SPF)	Spruce (SPF)	Spruce (SPF)
Section of the stud	38 x 89 mm	38 x 140 mm	38 x 140 mm	(38 x 89 mm)
Covering panel	12 mm Silicate board	15 mm Gypsum board	12 mm Silicate board	15 mm Gypsum board
Insulation material	Mineral wool	Mineral wool	Mineral wool	Mineral wool

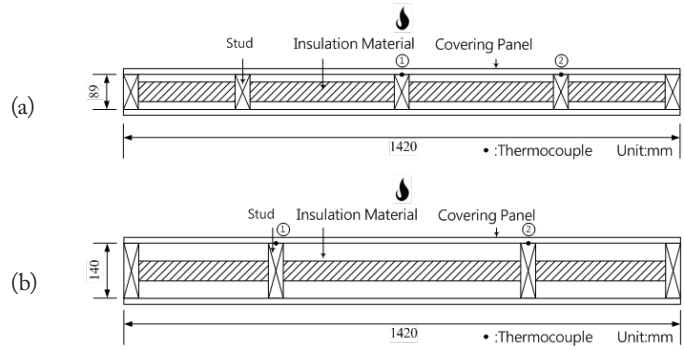

Fig. 1: WFWs and the positions of thermocouples for the pretests ((a): specimens A and D in Tab. 1; (b): specimens B and C in Tab. 1).

Fig. 2: ISO 834 Furnace used in this study.

Preliminary test results

As shown in Tab. 2, the temperatures measured at locations ① and ② (see Fig. 1 for the measurement point locations) on specimens A and C shown in Tab. 1 were averaged and used as the temperature condition for the CFS (S indicates silicate boards) fire scenario. Specimens A and C were made of the same surface material (silicate boards) but differed in wood stud size (the stud section depths were 89 and 140 mm for specimens A and C, respectively). Similarly, the temperatures measured at locations ① and ② (see Fig. 1 for the measurement point locations) on specimens B and D shown in Tab. 1 were averaged and used as the temperature condition for the CFG (G indicates gypsum boards) fire scenario. The surface heating curves of the wood studs tested in the CFS and CFG fire scenarios, as shown in Fig. 3, were used as the thermal boundary conditions for the subsequent principal test and the estimation of the charring depth.

Tab. 2: Temperature calculation for the CFS and CFG fire scenarios.

Fire scenario	Temperature calculation	Time to reach 300 °C	Max. temperature
CFS	[a](A1+A2+C1+C2)/4	19 min 50 s	702.5 °C
CFG	[b](B1+B2+D1+D2)/4	27 min 20 s	756.0°C

[a]The average temperature measured by thermocouples embedded at positions 1 and 2 of specimen A and those of specimen C (see Tab. 1 for A and C). [b]The average temperature measured by thermocouples embedded at positions 1 and 2 of specimen B and those of specimen D.

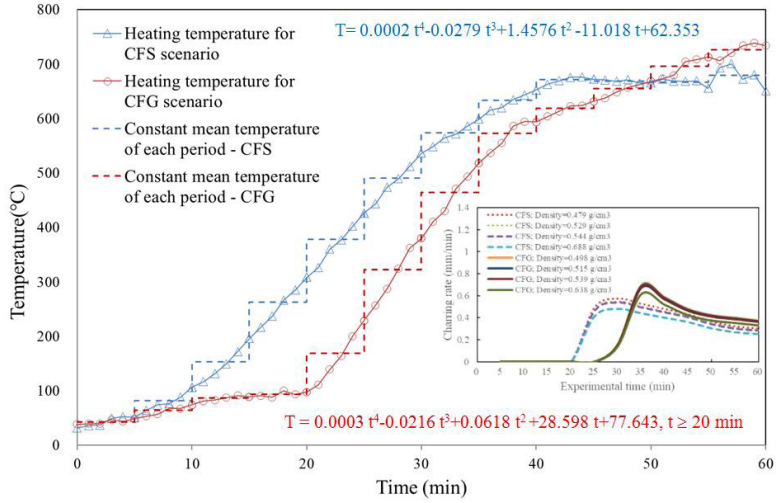

Fig. 3: The time–temperature curves and charring rate variations in the CFS and CFG fire scenarios for follow-up heat exposure experiments.

When wood is exposed to heat, a charred layer forms on its surface and provides thermal insulation. As the thickness of this charred layer increases, the insulation performance of the wood improves, the temperature increase slows and the charring rate decreases. The curve in Fig. 3 marked by △ depicts the increase in the surface temperature of the wood studs inside the CFS wall structures with a surface made of silicate boards when exposed to an ISO 834 fire. The surface temperature of the wood studs increased slowly during the first 5 min after the fire started and then increased rapidly between 5 and 40 min before stabilizing at approximately 660°C at 40 min. In addition, 20 min after the test began, the surface temperature of the wood studs inside the CFS wall structures exceeded 300 °C, and wood charring gradually started to occur inside the wood studs instead of at the stud surface (the location of the charring during the first 20 min).

The curve in Fig. 3 marked by ○ illustrates the increase in the surface temperature of the wood studs in the CFG wall structures with a surface composed of gypsum boards when exposed to an ISO 834 fire. The surface temperature of the wood studs increased slowly during the first 20 min after the fire started and then increased rapidly between 20 and 50 min (more rapidly than the surface temperature of the wood studs inside the CFS wall structure increased between 5 and 40 min after the fire started) before stabilizing at approximately 700°C at 50 min. In addition, the wood studs in the CFG wall structures started charring 28 min after the test began.

As demonstrated by the plot in the lower right corner of Fig. 3, the charring rate of the wood studs inside the CFS wall structures was close to 0 at the initial stage of the test and then started to increase rapidly at 20 min before peaking (at approximately 0.44 $mm \cdot min^{-1}$ – 0.50 $mm \cdot min^{-1}$) at 30 min. The charring rate then gradually decreased, reaching 0.25 $mm \cdot min^{-1}$ – 0.30 $mm \cdot min^{-1}$ at 60 min. The variation in the charring rate of the wood studs inside the CFG wall structures was similar to that of the wood studs inside the CFS wall structures. However, the charring rate of the wood studs inside the CFG wall structures started to increase 25 min after the test began, which was 5 min later than when the charring rate of the wood studs inside the CFG wall structures started to increase. Additionally, the charring rate for the CFG wall structures peaked (at approximately 0.61 $mm \cdot min^{-1}$ – 0.70 $mm \cdot min^{-1}$, slightly higher than the maximum charring rate of the wood studs inside the CFS wall structures) at 35 min and gradually decreased, reaching 0.33 $mm \cdot min^{-1}$ – 0.38 $mm \cdot min^{-1}$ at 60 min.

Tested wood studs and heat exposure experiments

In this study, wood stud specimens made of four common wood species used to produce wood studs, namely, Chinese fir (*Cunninghamia lanceolata*), Japanese cedar (*Cryptomeria japonica*), Southern pine (*Pinus* spp.) and spruce, were selected as principal test specimens. After being dried, these specimens each had moisture content below 19%. In addition, these specimens were trimmed to achieve a cross-sectional dimension of 14 x 14 cm. The Chinese fir, Japanese cedar, Southern pine and spruce specimens had an average density of 448 $kg \cdot m^{-3}$, 525 $kg \cdot m^{-3}$, 681 $kg \cdot m^{-3}$ and 551 $kg \cdot m^{-3}$, respectively. These specimens were each subjected to a heat exposure test in an electric furnace to simulate their conditions when exposed to a fire, as shown in Fig. 4. Inside the furnace, a heater was placed on each of the top, left and right sides. The two ends and bottom of each specimen were covered with a heat insulator, thereby allowing the other three sides (top and two lateral sides) to be heated evenly to simulate damage on three sides caused by a fire (i.e., after the covering plate fell off as a result of fire exposure (post-protection phase)). The air temperature inside the furnace was automatically increased based on Fig. 3 and recorded. Fig. 5 shows two specimens after the heating test. The test results were compared with predicted charring depths (see the next section for details).

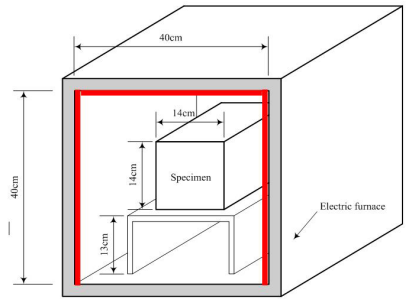

Fig. 4: A wood stud specimen placed in the furnace.

Fig. 5: Charred stud specimens after heat exposure experiments.

Prediction of the charring depth of the wood stud specimens

The charring depth of the wood stud specimens was predicted by substituting the principal test conditions (Fig. 3) into the correlation equations proposed by Hamada (1953) and Sugahara (1978) (hereinafter, the Hamada equation and the Sugahara equation). The predicted value of the charring depth of each specimen at 60 min was compared with the measured value. Eq. (1) shows the Hamada equation for predicting the charring depth of wood under isothermal heating boundary conditions:

$$x = a\left(\frac{T}{100} - 2.5\right)\sqrt{t} \tag{1}$$

where: x - charring depth (mm),
t - heat exposure time (min),
T - heating temperature (°C),
a - the constant with a value that depends on the wood type.

Eq. (2) shows the Sugahara equation for predicting the charring depth of wood under convective heating boundary conditions:

$$T = \left(T_f - T_a\right) erf(\eta) + T_a$$
$$\eta = \frac{X}{2\sqrt{\alpha t}},\ X = x + d,\ d = \frac{k}{h},\ \alpha = \frac{k}{\rho C} \tag{2}$$

where: T - temperature of the charring front (°C),
T_f - ambient temperature (°C),
T_a - initial temperature (°C),
erf(η) - complementary error function,
η - similarity variable,
x - charring depth (mm),
k - thermal conductivity (kcal·m^{-1}h^{-1}°C^{-1}),
h - convective heat transfer coefficient (kcal·m^{-2}h^{-1}°C^{-1}),
ρ - the density (kg·m^{-3}),
C - specific heat capacity (kcal·kg^{-1}°C^{-1}).

The charring depth of the wood stud specimens was estimated based on the above equations in conjunction with the standard heating curves proposed in this study (Fig. 3) using the following procedure.

1. Each time–temperature curve used to control the heating process was divided into several time segments, as shown in Fig. 3. The average temperature in each time segment was determined by averaging the corresponding heating temperatures.

2. The average charring rate and charring depth in a certain time segment were calculated using the Hamada and Sugahara equations, respectively, as shown in Fig. 6.

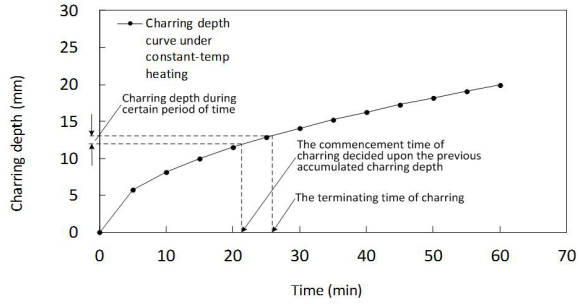

Fig. 6: Method of calculating the charring depth used in this study.

3. Based on the start time of charring defined in the previously mentioned step and the aforementioned time and location, the cumulative charring depth within a certain time segment was determined.

4. The variation in the charring depth of each wood stud specimen with time was then determined based on the sum of the charring depths in all the time segments.

RESULTS AND DISCUSSION

Relationship between the charring depth and density of the wood stud specimens

Fig. 7 shows the relationship between charring depth after 60 min of heating and the preheating density of the wood stud specimens. There was no significant correlation between the charring depth and preheating density. This finding is consistent with some existing results. Notably, Babrauskas (2005) concluded that studies of the effect of density on wood charring under ASTM E 119 or ISO 834 conditions have been inconsistent. Hugi et al. (2007) investigated the charring rates of 12 different wood species originating from Europe and the tropics with densities ranging from 350 $kg \cdot m^{-3}$ to 750 $kg \cdot m^{-3}$. The thickness of the charred layer was measured after a 30 min exposure to the standard ISO 834-1 fire. They found that no correlation between the charring rate and density. Yang et al. (2009) performed a series of heating tests of specimens of several wood species (Taiwania, Japanese cedar, Chinese fir, Douglas fir and Southern pine glulam) and found no significant correlation between the charring rate and wood density (correlation coefficient r: 0.53).

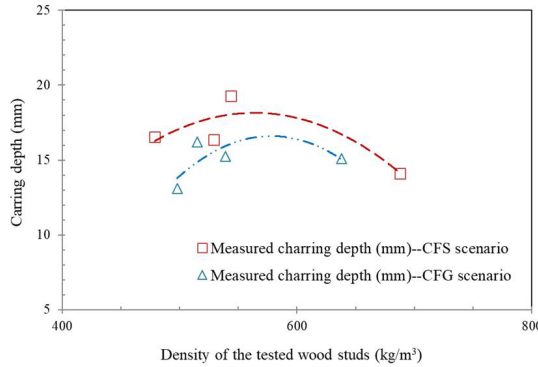

Fig. 7: The relationship among the charring depths (at 60 min) and densities of wood studs.

However, further analysis of the data shown in Fig. 7 indicates that there might be a parabolic relationship between charring depth and density. The charring depth first increased and then gradually decreased with increasing density. When the wood density was relatively low, the relatively large number of pores between wood fibers resulted in relatively lower thermal conductivity (k-effect). Consequently, the charring depth at 60 min was relatively small. As the density increased, the thermal conductivity increased, resulting in an increase in the charring depth. However, as the wood density increased, although the thermal conductivity increased, the combustion efficiency of the wood decreased as a result of the relatively dense structure (mass-effect). Consequently, the charring depth decreased. This is only a preliminary inference that requires validation with more data in the future.

Comparison of the predicted and measured values of charring depth

Fig. 8 shows a comparison of the predicted values of the charring depth of each specimen obtained using the Hamada (1953) and Sugahara (1978) equations (Eqs. 1 and 2, respectively) and the measured values. As demonstrated in Fig. 8, the predicted values obtained using the Hamada equation differed considerably from the measured values, whereas the predicted values obtained using the Sugahara equation were in good agreement with the measured values.

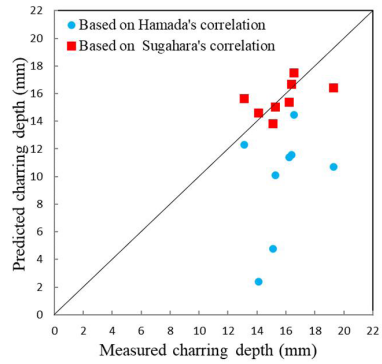

Fig. 8: The relationship between the experimental and predicted charring depths of four wood species (China fir, Japanese cedar, Southern pine and spruce).

In the Hamada equation for predicting the charring depth of wood (Eq. 1), the parameter a is obtained based on test results. The values of a are 1.0, 0.78 and 0.6 for Chinese fir, pine and cedar, respectively, which have densities ranging from 0.35 $g \cdot cm^{-3}$ to 0.5 $g \cdot cm^{-3}$. In addition, Hamada noted that the values of a for wood species with relatively high densities are relatively low. Our results show that for the charring depth of the wood stud specimens with densities ranging from 0.35 $g \cdot cm^{-3}$ to 0.5 $g \cdot cm^{-3}$, the predicted values obtained using the Hamada equation were relatively close to the measured values. For example, the r value between the predicted and measured values of the charring depth of the Chinese fir wood stud specimens (density: 0.4 $g \cdot cm^{-3}$ - 0.5 $g \cdot cm^{-3}$) was 0.86. For the charring depth of the wood stud specimens with a density higher than 0.5 $g \cdot cm^{-3}$, the predicted values considerably differed from the measured values. For example, the r value between the predicted and measured values of the charring depth of Southern pine specimens (density: 0.63 $g \cdot cm^{-3}$ - 0.71 $g \cdot cm^{-3}$) was only 0.59.

Overall, the predicted values obtained using the Sugahara equations were relatively close to the measured values (average r: 0.83). In addition to density, the Sugahara equation contains the coefficient of heat convection. Because the accounts for the convection of hot air resulting from a fire, the Sugahara equation aligns with the use of an actual fire as thermal boundary conditions in this study. As a result, the predicted values obtained using the Sugahara equations were very close to the measured values.

CONCLUSIONS

In this study, the variation in the surface temperature of wood studs inside WFWs with time was determined based on ISO 834 fire-resistance tests, and the resultant heating conditions were used in the subsequent heat exposure test. Then, wood stud specimens of four wood species (Chinese fir, Japanese cedar, Southern pine and spruce) were each subjected to a heat exposure test in an electric furnace. This study investigated the charring depth of woods studs inside WFWs in a fire. The results derived from this study can be summarized as follows:

1. There was no significant difference in the charring depth at the top and on the lateral sides of all specimens made of the same wood species under the same heating conditions.
2. There was an insignificant correlation between the charring depth and density of the wood stud specimens.
3. For the predicted values of the charring depth obtained using the Hamada equation, only those of the wood stud specimens with densities in the range of 0.35 $g \cdot cm^{-3}$ - 0.5 $g \cdot cm^{-3}$ were relatively close to the measured values.
4. For the predicted values of the charring depth obtained using the Sugahara equation, those of the wood stud specimens with densities in the range of 0.4 $g \cdot cm^{-3}$ - 0.72 $g \cdot cm^{-3}$ were very close to the measured values. Thus, Sugahara equation is recommended to be used to predict the charring depth of woods studs inside WFWs in a fire.

ACKNOWLEDGMENTS

The support from the Architecture and Building Research Institute, Ministry of the Interior, Taiwan, in this study is gratefully acknowledged.

REFERENCES

1. ASTM E 119, 2018: Standard test methods for fire tests of building construction and materials.
2. Babrauskas, V., 2005: Charring rate of wood as a tool for fire investigation. Fire Safety Journal 40(6): 528-554.
3. Frangi, A., Erchinger, C., Fontana, M., 2008: Charring model for timber frame floor assemblies with void cavities. Fire Safety Journal 43(8): 551-564.
4. Hamada, M., 1953: Wood burning rate. Proc. Jpn. Soc. Fire 2: 106-107.
5. Hugi, E., Wuersch, M., Risi, W., Wakili, K.G., 2007: Correlation between charring rate and oxygen permeability for 12 different wood species. Journal of Wood Science 53(1): 71-75.
6. ISO 834-1, 1999: Fire resistance tests – Elements of buildings construction. Part-1: General Requirements.
7. ISO 834-8, 2002: Fire-resistance tests – Elements of building construction. Part 8: Specific requirements for non-load bearing vertical separating elements.
8. Jefimovas, A., Mačiulaitis, R., Sikarskas, D., 2017: Prediction of temperature of standard fire exposure. Journal of Civil Engineering and Management 23(4): 533-540.
9. Kolaitis, D.I., Asimakopoulou, E.K., Founti, M.A., 2014: Fire protection of light and massive timber elements using gypsum plasterboards and wood based panels: a large-scale compartment fire test. Construction and Building Materials 73: 163-170.
10. Li, K.Y., Wang, J., Ji, J., 2014: An experimental investigation on char pattern and depth at post flashover compartments using medium-density fibreboard (MDF). Fire and Materials 40(3): 368-384.
11. Lineham, S.A., Thomson, D., Bartlett, A.I., Bisby, L.A., Hadden, R.M., 2016: Structural response of fire-exposed cross-laminated timber beams under sustained loads. Fire Safety Journal 85: 23-34.
12. Östman, B., Brandon, D., Frantzich, H., 2017: Fire safety engineering in timber buildings. Fire Safety Journal 91: 11-20.
13. Peng, L., Hadjisophocleous, G., Mehaffey, J., Mohammad, M., 2010: Fire resistance performance of unprotected wood–wood–wood and wood–steel–wood connections: a literature review and new data correlations. Fire Safety Journal 45(6-8): 392-399.
14. Sugahara, S., 1978: Study of wood carbonization rate. Summaries of technical papers of annual meeting. Archit. Inst. Jpn. : 2109-2110.
15. Xu, Q., Chen, L., Harries, K.A., Zhang, F., Liu, Q., Feng, J., 2015: Combustion and charring properties of five common constructional wood species from cone calorimeter tests. Construction and Building Materials 96: 416-427.
16. Yang, T.H., Wang, S.Y., Tsai, M.J., Lin, C.Y., 2009: The charring depth and charring rate of glued laminated timber after a standard fire exposure test. Building and Environment 44(2): 231-236.

Hung-Chi Su
Architecture and Building Research Institute
Ministry of The Interior
New Taipei City 23143
Taiwan

Shu-Fen Tung, Chun-Ta Tzeng
National Cheng Kung University
Department of Architecture
Tainan City, 701
Taiwan

*Chi-Ming Lai
National Cheng Kung University
Department of Civil Engineering
Taiwan
1, University Road
Tainan City, 701
Taiwan
Phone: +886-6-2757575 Ext. 63136
*Corresponding author: cmlai@mail.ncku.edu.tw